Article

Step-Economical Photoassisted Diversity-Oriented Synthesis: Sustaining Cascade Photoreactions in Oxalyl Anilides to Access Complex Polyheterocyclic Molecular Architectures

Dmitry M Kuznetsov, and Andrei G. Kutateladze

J. Am. Chem. Soc., **Just Accepted Manuscript** • Publication Date (Web): 20 Oct 2017

Step-Economical Photoassisted Diversity-Oriented Synthesis: Sustaining Cascade Photoreactions in Oxalyl Anilides to Access Complex Polyheterocyclic Molecular Architectures

Dmitry M. Kuznetsov and Andrei G. Kutateladze*

Department of Chemistry and Biochemistry, University of Denver, Denver, CO 80208.

ABSTRACT: Atom- and step-economy in photoassisted DOS is achieved with a versatile oxalyl linker offering rapid access to complex alkaloid mimics in very few experimentally simple steps: (i) it allows for fast tethering of the photoactive core to the unsaturated pendants, especially important in the case of (hetero)aromatic amines – essentially a one pot reaction with no isolation of intermediates; (ii) the α-dicarbonyl tether acts as a chromophore enhancer, extending the conjugation chain and facilitating the 'harvest' of the lower energy photons for the primary and secondary photoreactions, (iii) it enhances the quantum yield of intersystem crossing (ISC), i.e. it is capable of sensitizing secondary photochemical processes in the cascade and, (iv) the tether forms an additional heterocyclic moiety, imidazolidine-4,5-dione, a known pharmacophore. The overall photoassisted cascade is an efficient complexity-building process as quantified by computed step-normalized complexity indices, leading to extended polyheterocyclic molecular architectures comparable in complexity to natural products such as paclitaxel while requiring only 2-4 simple synthetic steps from readily available chemical feedstock.

1. INTRODUCTION

The quest for rapid growth of molecular complexity in synthetic organic chemistry continues, whether the subject at hand is the target- or diversity-oriented,[1] or function-oriented[2] synthesis. The general notion of step-economy and various other economies of synthesis[3] is particularly central here and now is also quantifiable, especially with the modern computer-aided estimates of step-normalized increase in molecular complexity indices.[4]

In recent reviews by Porco and Stephenson,[5] or Remi and Bochet,[6] photochemistry – and especially photoinduced cycloadditions – are shown to offer expedited access to complex chemotypes where ground state reactions are at best challenging if not impossible.[7] Needless to say we fully share this philosophy. Earlier we developed a general photoassisted synthetic methodology for rapid generation of molecular complexity and diversity in nitrogen-containing polyheterocycles based on a short, three-four steps, synthetic sequence involving (i) experimentally simple modular assembly of photoprecursors, reminiscent of multicomponent reactions in simplicity (ii) key photochemical step to construct the core scaffold, accompanied by significant growth of complexity and (iii) postphotochemical modification to further diversify the target.[8] This expedited access to rather complex molecular architectures takes advantage of excited state intramolecular proton transfer (ESIPT) in aromatic amino ketones via the intermediacy of aza-*o*-xylylenes. Recently we have shown that aza-*o*-xylylenes are capable of dearomatizing appropriately tethered benzenoid aromatic moieties in an unprecedented [2+4] photoreaction topology leading to privileged scaffolds such as tetrahydroquinolines fused to cyclohexadiene moiety.[9] As the primary photoprocess occurs in the triplet state[10] we hypothesized that a secondary excitation and intersystem crossing into the triplet manifold could be even more advantageous synthetically, given the expected eventual localization of the triplet on the diene moiety as dienes are the known "sinks" for triplet energy.[11]

This rationale of setting up a complex synthetically useful photochemical cascade required re-thinking the role of the tether utilized in the "assembly" of linear photoprecursors. In sum, we sought a multi-functional compact tether which would (i) allow for straightforward and efficient modular "assembly" of linear photoprecursors from readily available chemical feedstock; (ii) extend the conjugation in the primary chromophores, i.e. *o*-aminoketones, and therefore enhance their light-harvesting properties; (iii) enhance UV absorption of the primary photoproducts paving the way for ready re-excitation; (iv) facilitate fast intersystem crossing, ISC, into the triplet manifold at the *secondary* step of the photochemical cascade; and finally, (v) as the linker becomes an additional heterocyclic moiety, ideally it would form/enhance the potential pharmacophore.[12]

In this paper, we report one solution under which all these conditions are met based on the oxalyl amide tether, resulting from a stepwise "fastening" of two aniline moieties with oxalyl chloride, which can be carried out in a 'one-pot' fashion. As we show below this experimentally simple modular assembly of photoprecursors offers a straightforward entry into the cascade photochemical synthetic sequence leading to polyheterocyclic secondary photoproducts suitable for short postphotochemical transformations to yield complex alkaloid mimics.

2. RESULTS AND DISCUSSION

2.1. Two-step photocascade

Non-symmetric oxalyl anilide photoprecursors were readily accessed via a stepwise reaction with oxalyl chloride as shown in Scheme 1. This scheme also illustrates a typical primary photoreaction initiated by ESIPT in the photoactive *o*-amido ketone

chromophore. The generated triplet aza-*o*-xylylenes were capable of dearomatizing the tethered anilide moiety, yielding cyclohexadiene-fused tetrahydroquinolines as primary photoproducts.

Scheme 1. Assembly of non-symmetric oxalyl anilide precursors and a typical ESIPT-mediated primary photoreaction leading to dearomatization of tethered anilide.

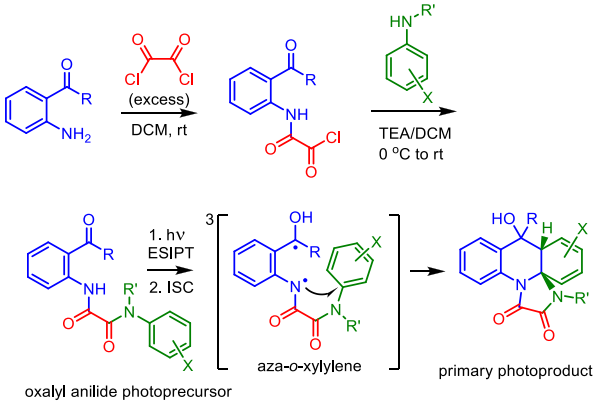

Such cycloadditions of aza-*o*-xylylenes generally reduce UV absorption of the primary photoproducts, mostly due to deconjugation of the aromatic carbonyl group, which becomes benzylic alcohol. However, oxalylamide-based primary photoproducts possess extended conjugation and by design are capable of secondary photoexcitation. This was indeed observed. When oxalylamidobenzaldehyde precursor **1a** was irradiated with UV LEDs @ 365nm, the initially formed primary photoproduct **2a** was depleted upon extended irradiation to yield polyheterocyclic **3a** possessing 2-azabicyclo[2.2.2]octene moiety.

Scheme 2. Photochemical cascade with a secondary reaction sensitized by the multifunctional tether.

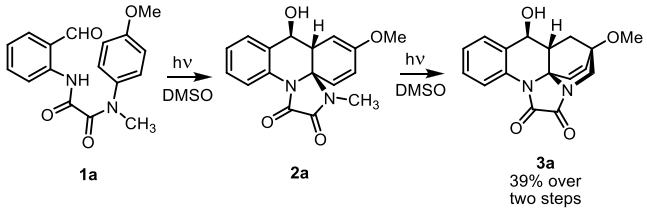

This newly discovered photochemical cascade is accompanied by a considerable increase of molecular complexity in one experimentally simple step. The reaction was consistently reproduced on a broad range of substrates possessing additional alicyclic and heterocyclic functionalities, Table 1. These photoprecursors are readily diversified based on reductive amination of anisidine or similar anilines with various aliphatic, aromatic, or heteroaromatic aldehydes followed by amide coupling and other experimentally simple procedures similar to those depicted in Scheme 1. For example, starting with 5-aminoindolinone and nicotinaldehyde one gains rapid access to photoprecursor **1i** which upon irradiation yields two regioisomers **3i** and **3i'** in a stereospecific fashion with the former polyheterocycle **3i** possessing five new contiguous stereogenic centers. Typical irradiation conditions included a 100 mg scale (2.5 mM solution) with seven 2.9W @ 365 nm UV LEDs for 2.5-8 hours for aminobenzaldehydes or 13-32 hours for aminoacetophenones.

Table 1. Products of the two-step photo-cascade

Photoprecursor	Secondary Photoproduct(s)	
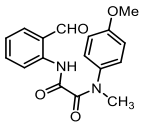 **1a**	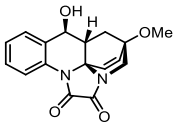 **3a** (39%)[a]	
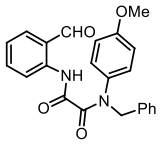 **1b**	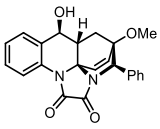 **3b** (35%)	
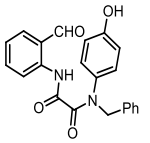 **1c**	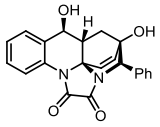 **3c** (62%)	
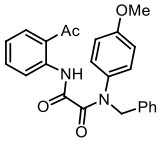 **1d**	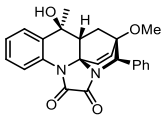 **3d** (40%)	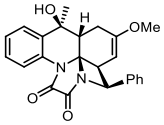 **3d"** (trace amounts)
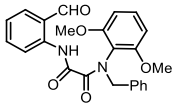 **1e**	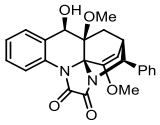 **3e** (75%)	
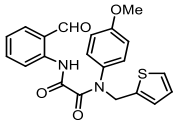 **1f**	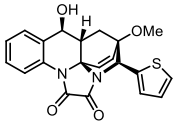 **3f** (36%)	
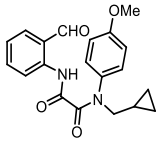 **1g**	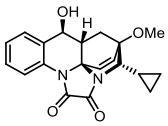 **3g** (48%)	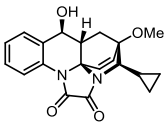 **3g'** (9%)
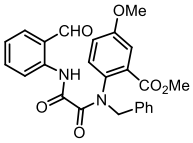 **1h**	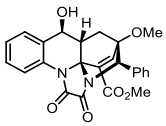 **3h** (50%)	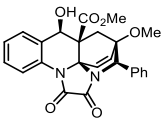 **3h'** (33%)
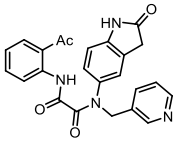 **1i**	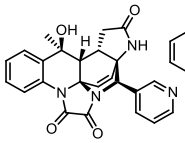 **3i** (40%)	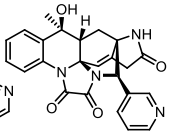 **3i'** (30%)

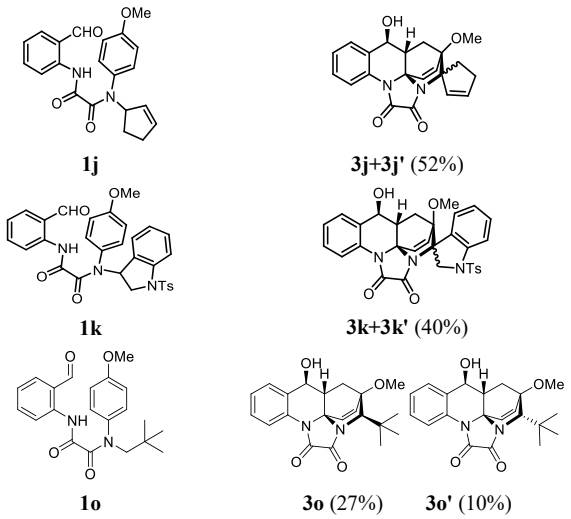

[a]isolated yields after two steps

2.2. Mechanistic Rationale.

Unlike our previous dearomatization reaction with phenol-based photoprecursors which yielded both *syn*- (major) and *anti*-diastereomeric benzylic alcohols (the *syn-/anti*- nomenclature refers to the relationship between the benzylic OH group and the cyclohexadiene moiety),[9] photo cascade in anilides **1** produced exclusively *anti*-isomers. After ESIPT, the initial triplet diradical, Figure 1, is born in the *in*-OH conformation, which is stabilized by the shown intramolecular hydrogen bonding (blue dashed lines). As the *syn*-isomer could only be originated from the *out*-OH rotamer stabilized by a hydrogen bond to solvent, we hypothesize that oxalylamides form much stronger intramolecular hydrogen bonds and, therefore, significantly bias the stereochemical outcome toward the observed *anti*- products. Figure 1 illustrates that either clockwise or anti-clockwise rotation around the Ar-N bond in the *in*-OH conformer produces two enantiomers of the *anti*-diastereomer, as long as the intramolecular H-bonding persists. This intramolecular H-bond could be either between the OH group and the nitrogen atom or amide's carbonyl as shown.

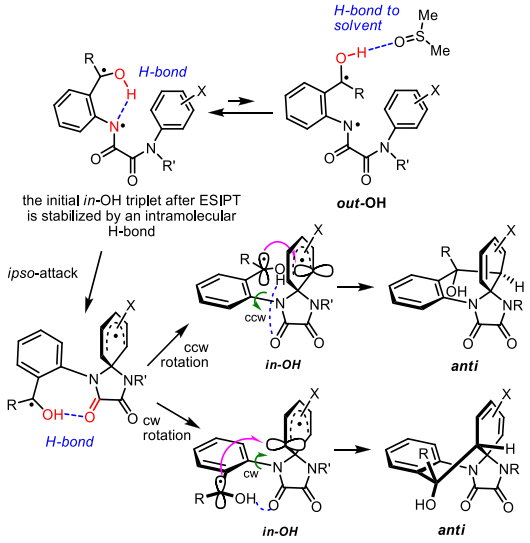

Figure 1. *Anti*-diastereoselectivity of the primary photo dearomatization is rationalized in terms of strong intramolecular H-bonding maintaining the *in*-OH conformation in the initial diradical.

The secondary photoreaction in the photo cascade, Figure 2, conceivably involves excitation of the oxalyl anilide chromophore, intersystem crossing into the triplet manifold with triplet energy transfer from the dicarbonyl moiety to cyclohexadiene, followed by aliphatic α-hydrogen abstraction and recombination of two radical centers after ISC to complete the formation of the azabicyclo[2.2.2]octene core. This rationale is supported by the DFT calculations, B3LYP/6-311+G(d,p). We were able to identify the initial $\mathbf{T_2}$ state which is localized on the α-dicarbonyl chromophore (69.9 kcal/mol relative to the ground state of the primary photoproduct **2a**). The lowest triplet state, $\mathbf{T_1}$ (49.7 kcal/mol) is localized on the cyclohexadiene moiety as expected. Instructively, the critical H-atom transfer is an exergonic step on the triplet hypersurface, with the triplet diradical **DR** $\mathbf{T_1}$ being approximately 8 kcal/mol 'downhill.' This exergonicity is not entirely unexpected, as the triplet cyclohexadiene is transitioned into two conjugated radicals, the methoxyallyl radical and the $ArNC(O)C(O)N\text{-}CH_2^{\bullet}$ radical. Analysis of Mulliken spin density in the amidomethyl radical supports the delocalization hypothesis, with the adjacent carbonyl oxygen carrying 0.15 of alpha spin density (in addition to 0.84 residing on the methylene carbon).

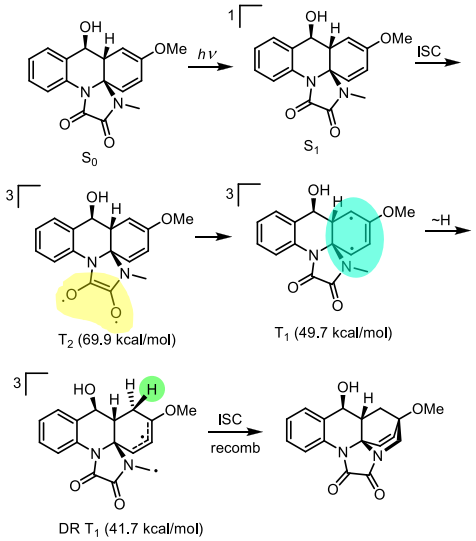

Figure 2. Plausible mechanism for the secondary step in the photochemical cascade (relative DFT B3LYP/6-311+G(d,p) energies are in parentheses).

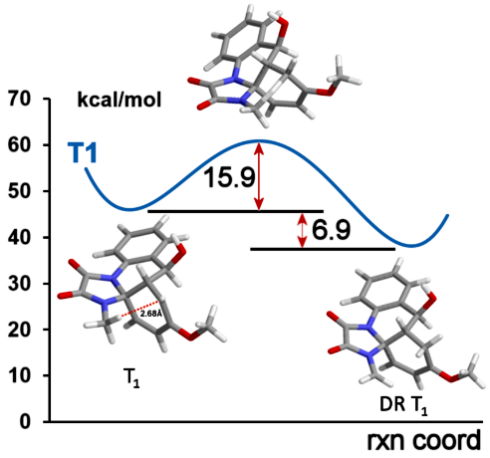

Figure 3. Triplet energy profile for the H atom transfer: ZPE-corrected B3LYP/6-311+G(d,p) DFT energies.

In the case of acetophenone-based photoprecursor **1d** we isolated a very small amount of diaza-benzofenestrane **3d"**, which was characterized by x-ray.[13,14] Isolation of **3d"** offers additional support for the biradical mechanism, with **DR T₁** recombining at the alternative terminus of the allylic radical.

ZPE-corrected energy of the transition state for the critical hydrogen atom transfer, Figure 3, revealed a small activation barrier of only 15.9 kcal/mol, which explains the relatively fast reaction rate at ambient temperature. Fully optimized structure of cyclohexadiene-localized triplet **T₁** also revealed very short distance for hydrogen transfer, Figure 3.

To further support this triplet diradical mechanism the relative quantum yields of the protic and deuterated substrates **2a/2a**-d_3 at 23 °C were compared with the expectation of a primary isotope effect. The actual experimental value that we obtained, Φ_H/Φ_D = 72 ± 12, implied quantum tunneling, Figure 4A.

(A)

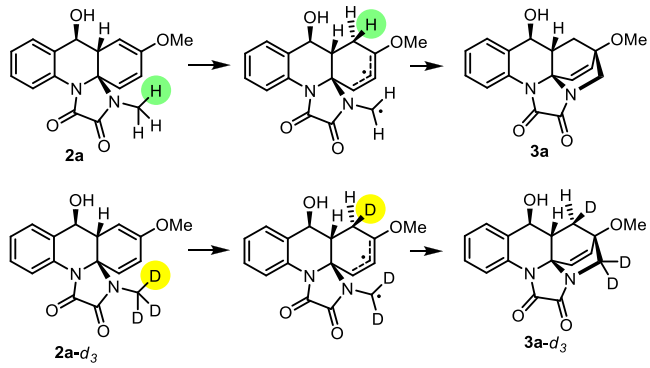

Φ_H/Φ_D = 72 ± 12

(B)

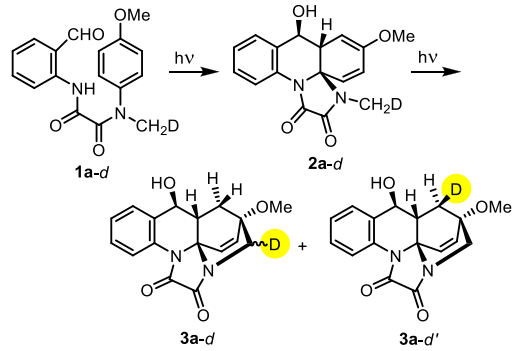

Φ_H/Φ_D = 34 ± 14

Figure 4. Deuterium isotope effect on quantum yields of production of **3a** from **1a**.

As the transformation of **1a** to **3a** is a multistep process involving singlet and triplet excited states, we considered that the cumulative isotope effect on the quantum yield of production of **3a** could potentially reflect contributions from isotope effects on lifetimes of the excited species along the reaction coordinate, in which case the kinetic isotope effect on the actual H atom transfer step could be very different. To clarify this point and rule out isotope effects on the lifetimes, we synthesized monodeuterated **1a**-*d*, Figure 4B, and determined the deuterium distribution in the resulting **3a**-*d*. After statistical correction for two protons *vs* one deuterium atom, we arrived at a lower ratio Φ_H/Φ_D = 34 ± 14. Based on this result we rationalize that there is a small isotope effect on lifetimes of excited species in the previous example, Figure 4A. At the same time this large isotope effect of 34 obtained at ambient temperature, which exceeds the expected value for a primary isotope effect by a factor of four, offers proof that hydrogen atom transfer in excited **2a** does occur via quantum tunneling. These large room temperature values are not unprecedented: KIEs of 5-55 have been observed before for the proton-transfer step in methylamine dehydrogenase.[15] Hydrogen atom tunneling in the excited states is also precedented, but mostly studied for hydrogen abstraction by carbonyls.[16]

The cyclopropyl radical clock (in **1g**) indicates that **DR T₁** is probably too short-lived and collapses fast following ISC to form products **3g** and **3g'** with the cyclopropane probe intact. Also, with the exception of the N-methyl substituted **1a**, all other substrates (i.e. N-CH_n-R substituted amides) expectedly exhibited very fast H atom transfer due to additional radical stabilization by R, especially by aromatic or olefinic substituents. In all these cases, the primary photoproducts **2** are barely detectable in the reaction mixture as the H-transfer step is much faster than the first photochemical step, so only azabicyclo[2.2.2]octenes **3** dominate the products.

Formation of tertiary alcohol **3c** from free phenol **1c** in good yield (62% over two steps) is another instructive example of the efficiency of the secondary photochemical step, Scheme 3. The primary photoproduct in this case, dienol **2c**, is re-excited and efficiently engaged in the second step of the photo cascade to yield azabicyclo[2.2.2]octene **3c**. An alternative reaction, tautomerization of dienol **2c** into the corresponding enone was not observed.

Scheme 3. Free aminophenol precursor 1c yields dienol 2c photoconverted into azabicyclo[2.2.2]octene 3c instead of tautomerization into enone.

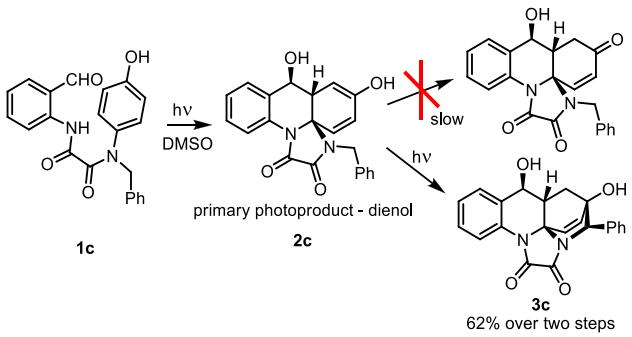

2.3. Postphotochemical transformations.

From the synthetic standpoint, this photoinduced cascade including the dearomatization followed by the azabicycle formation, produces new complex polyheterocyclic cores which are readily decorated with additional functionalities or hetero/alicyclic pendants via experimentally simple tweaking of the starting photoprecursors.

Topologically, *there is another critical point to highlight*: this two-step process brings the *para*- extremities of the initial aromatic system into the close proximity of each other, Figure 5, which we exploited for simple and straightforward postphotochemical modifications.

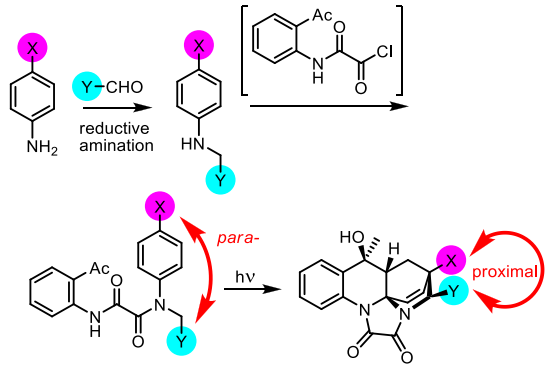

Figure 5. Topology of the two-step photocascade: bringing the *para*-substituents into the *vicinal* relationship.

Scheme 4A illustrates this point with the acid-catalyzed formation of 7-azaindole **4** from photoprecursor **1l** 'assembled' from *o*-aminoacetophenone, mono Boc-protected *p*-phenylenediamine, and 2-fluoro-nicotinaldehyde. Scheme 4B shows that the photoinduced topological change, which brings an amine into the proximity of methyl carboxylate in **3m**, offers an opportunity to access lactam **5**. Another example is the Pictet-Spengler reaction, which is readily set to fuse an additional tetrahydroquinoline moiety to the already complex polyheterocyclic core of the primary photoproduct **3n**, Scheme 4C.

Scheme 4. Postphotochemical modifications of the primary photoproducts via one additional step.

(A)

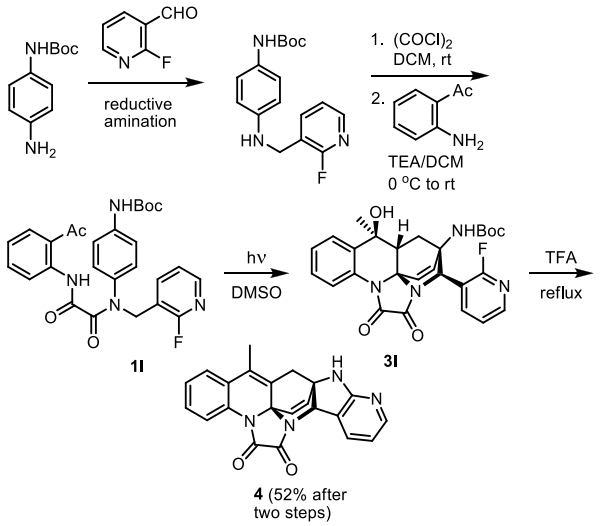

(B)

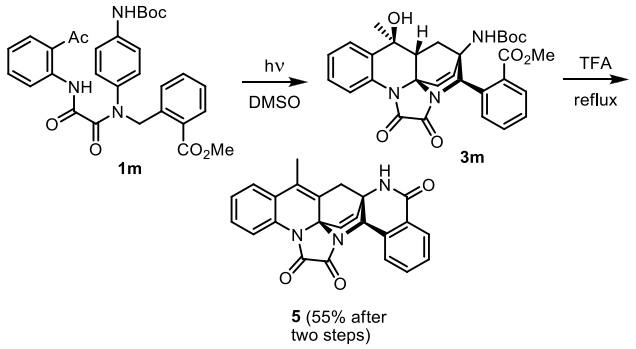

(C)

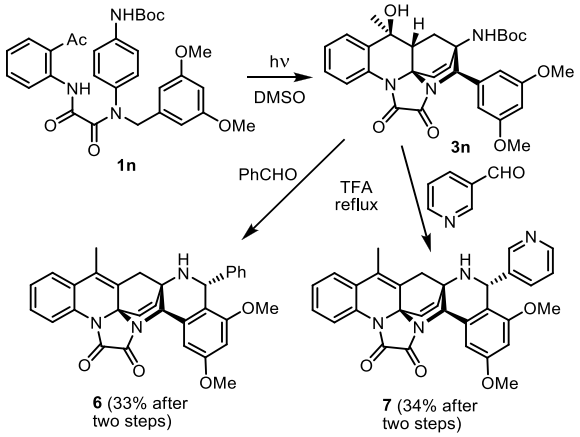

These short and experimentally simple procedures are accompanied by a considerable increase of complexity after each photochemical and postphotochemical step, attesting to the preparative value of the method: while the yields are moderate, they are achieved in 3-4 steps from readily available chemical feedstock. It is also easy to see that examples in Scheme 4 produce two double bonds suitable for an additional one-step functionalizations. Due to significantly different reactivity of styrenic *vs* azabicyclo[2.2.2]octene moieties, these double bonds are "addressable," i.e. can be selectively engaged with electrophiles or 1,3-dipoles.

Scheme 5 shows that two double bonds of diene **8**, prepared by postphotochemical dehydration of photoproduct **3b** in refluxing TFA, differ in reactivity to the extent that they are "addressable" with different reagents. For example, epoxidation of

8 is directed at its styrenic alkene yielding epoxide **9** in 27% yield over three steps. In contrast, the 1,3-dipolar cycloaddition of benzonitrile-oxide affects the azabicyclo[2.2.2]octene moiety furnishing isoxazoline **10** and a product of double addition **11**. Similar bis dipolar cycloadditions yielding isoxazolo-isoxazolidines, such as **11**, are precedented in the literature. [17]

This difference in reactivity of the two double bonds could be rationalized in terms of hyperconjugative deactivation of the azabicyclo[2.2.2]octene moiety via the $\pi \rightarrow \sigma^*_{CN}$ interaction, depleting it of the π density. On the other hand, the styrenic double bond is more nucleophilic due to the electron-donating *ortho*-nitrogen, given that in this rigid molecular framework its lone pair does not overlap well with the carbonyl. This could be another example of a stereoelectronic chameleon described recently.[18]

Scheme 5. Chemoselectivity of alkenic moieties in dehydrated photoproducts.

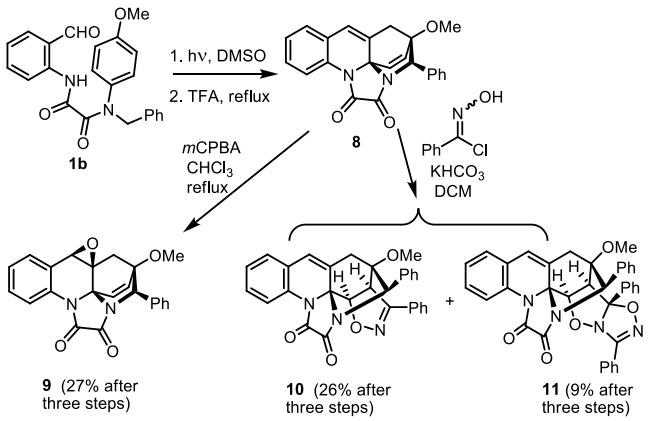

ESIPT-based generation of aza-*o*-xylylenes and subsequent dearomatization of tethered benzenoid aromatics require polar solvents, such as DMSO, for the efficient photochemical cascade. However, DMSO is not a suitable solvent for the post-photochemical 1,3-dipolar cycloadditions, for example, the ones shown in Scheme 5. Replacing DMSO with DMF offered an opportunity to implement a one-pot synthesis of heterocycles such as **12** directly from photoprecursors, Scheme 6. Again, this experimentally simple one-pot procedure diastereoselectively sets *seven* contiguous stereogenic centers in a complex nitrogen polyheterocycle.

Scheme 6. One-pot implementation of the ESIPT-based photoassisted cascade with postphotochemical modifications.

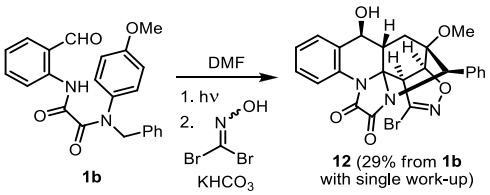

2.4. Molecular Complexity

Molecular complexity was quantified using the DataWarrior (Actelion Pharmaceuticals Ltd.) software.[4c] As Figure 6 illustrates, photoprecursors **1** have complexity indices similar to the initial feedstock chemicals, such as carboxaldehydes used for reductive amination with anisidines or *p*-phenylenediamine, and also *o*-aminoacetophenone which makes up the photoactive ESIPT core. In contrast, the photoassisted cascade accounts for a dramatic increase of complexity, which puts photoproducts – obtained in a total of two-four experimentally easy steps – in the same league as paclitaxel, while possessing much smaller molecular weight.

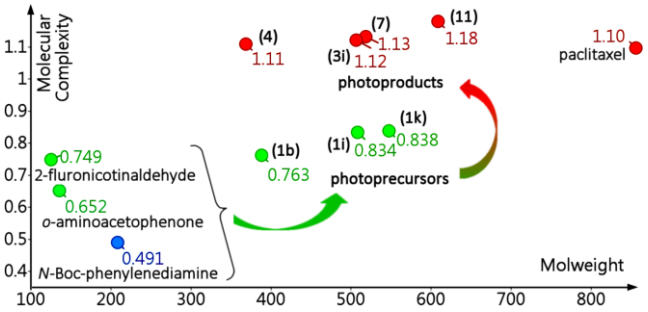

Figure 6. Molecular complexity graph for selected starting materials and photoproducts (numerical labels show calculated molecular complexity indices as defined in DataWarrior 4.6.0, Osiris).

The increase of molecular complexity per step is one important metric, particularly in the context of developing new photoassisted DOS methodologies. We also note that other DataWarrior's metrics such as druglikeness or drugscore are also favorable for the new alkaloid mimics. For example, drugscore for 7-azaindole **4**, 0.46, exceeds the calculated value for paclitaxel, 0.24, almost by a factor of two.

3. CONCLUSIONS

We have developed a robust photoassisted methodology for rapid access to complex alkaloid-like polyheterocyclic molecular architectures, which involves photochemical two-step cascade as a key step. With photoprecursors assembled from readily available chemical feedstock via experimentally simple procedures this overall synthetic DOS strategy is centered around the multifunctional oxalylamide tether, which improves photophysical properties of the precursor and the primary photoproduct alike, and effectively sensitizes synthetically useful secondary photoreactions. Subsequent, one-two step experimentally simple postphotochemical modifications take advantage of the reactive functionalities installed in the photochemical step and allow for further growth of complexity and diversity of the products. The key step, dearomatization of the tethered anilide moiety by the triplet aza-*o*-xylylene generated via ESIPT, produces a tetrahydroquinoline fused to cyclohexadiene fragment. The secondary photochemical step utilizes the low triplet energy of the diene, rendering this a general strategy for generation of tetrahydroquinoline cores with fused aza-bicyclo[2.2.2]octene. The formation of the bicyclo[2.2.2]octene moiety occurs via hydrogen atom transfer from the α-position in N-CH_n-R to the triplet diene. The isotope effect on the relative quantum yields of formation of the secondary photoproduct reveal that this hydrogen atom transfer occurs via quantum tunneling.

ASSOCIATED CONTENT

Supporting Information. Experimental details. This material is available free of charge via the Internet at http://pubs.acs.org.

AUTHOR INFORMATION

Corresponding Author

*E-mail: akutatel@du.edu
ORCID: 0000-0003-3066-517X

Notes

The author declare no competing financial interest.

ACKNOWLEDGMENT

This paper is dedicated to Al Padwa, a mentor and friend, on the occasion of his 80th birthday.

This research is supported by the NSF, CHE-1362959. We thank Bruce Noll, Bruker AXS Inc, for help with solving a difficult xray structure of compound **6**.

REFERENCES

(1) Schreiber, S. L. *Science*, **2000**, *287*, 1964.

(2) (a) Wender, P.A.; Quiroz, R.V.; Stevens, M. C. *Acc. Chem. Res.* **2015**, *48*, 752. (b) Wender, P.A.; Verma, V A.; Paxton,, T. J.; Pillow, T. H. *Acc. Chem. Res.* **2008**, *41*, 40.

(3) Newhouse, T.; Baran, P. S.; Hoffmann, R. W. *Chem. Soc. Rev.* **2009**, *38*, 3010.

(4) (a) the first general index of molecular complexity was developed by Bertz, S. H. *J. Am. Chem. Soc.* **1981**, *103*, 3599. (b) for the most recent overview of various methods to define molecular complexity and the many roles of molecular complexity in drug discovery see Méndez-Lucio, O.; Medina-Franco, J. L. *Drug Disc. Today* **2017**, *22*, 120. (c) we are aware of two computational sources available in the public domain for evaluating molecular complexity indices: PubChem (https://pubchem.ncbi.nlm.nih.gov) and DataWarrior (http://openmolecules.org/datawarrior) developed by Actelion Pharmaceuticals Ltd.

(5) Kärkäs, M. D.; Porco, J. A. Jr.; Stephenson, C. R. J. *Chem. Rev.* **2016**, *116*, 9683.

(6) Remy. R.; Bochet, C. G. *Chem. Rev.* **2016**, *116*, 9816.

(7) Triplet state cycloadditions are also well-precedented, selected examples: (a) Wagner P. J. *Acc. Chem. Res.* **2001**, *34*, 1. (b) Griesbeck, A. G.; Stadtmüller, S. *J. Am. Chem. Soc.* **1990**, *112*, 1281 (c) Zeidan, T. A.; Kovalenko, S. V.; Manoharan, M.; Clark, R. J.; Ghiviriga, I.; Alabugin, I. V. *J. Am. Chem. Soc.* **2005**, *127,* 4270.

(8) (a) O. A. Mukhina, N. N. B. Kumar, T. M. Arisco, R. A. Valiulin, G. A. Metzel, A. G. Kutateladze, *Angew. Chem., Int. Ed.* **2011**, *50*, 9423. (b) N. S. Nandurkar, N. N. B. Kumar, O. A. Mukhina, A. G. Kutateladze, *ACS Comb. Sci.* **2013**, *15*, 73. (c) N. N. B. Kumar, O. A. Mukhina, A. G. Kutateladze, *J. Am. Chem. Soc.*, **2013**, *135*, 9608. (d) W. C. Cronk, O. A. Mukhina, A. G. Kutateladze, *J. Org. Chem.*, **2014**, *79*, 1235. (e) N. N. B. Kumar, D. M. Kuznetsov, A. G. Kutateladze, *Org. Lett.*, **2015**, *17*, 438. (f) O. A. Mukhina, N. N. B. Kumar, T. M. Cowger, A. G. Kutateladze, *J. Org. Chem.*, **2014**, *79*, 10956. (g) W. J. Umstead, O. A. Mukhina, A. G. Kutateladze, *Eur. J. Org. Chem.*, **2015**, 2205. (h) W. J. Umstead, O. A. Mukhina, A. G. Kutateladze, *Aust. J. Chem.* **2015**, *68*, 1672. (i) O. A. Mukhina, D. M. Kuznetsov, T. M. Cowger, A. G. Kutateladze, *Angew. Chem. Int. Ed.*, **2015**, *39*, 11516.

(9) Kuznetsov, D.M.; Mukhina, O.A.; Kutateladze, A.G. *Angew. Chem.*, **2016**, *55*, 6988.

(10) Mukhina, O.A.; Cronk, W.C.; Kumar, N.N.B.; Sekhar, M.; Samanta, A.; Kutateladze, A.G. *J. Phys. Chem. A.*, **2014**, *118*, 10487.

(11) (a) Wagner, P. J. *J. Am. Chem. Soc.* **1967**, *89*, 5715. (b) Dalton, J. C.; Turro, N. J.; *Annu. Rev. Phys. Chem.* **1970**, *21*, 499. (c) Wagner, P. J. *Acc. Chem. Res.* **1971**, *4*, 1681. (d) Barltrop, J. A.; Carless, H. A. J. *J. Am. Chem. Soc.* **1971**, *93*, 4794. (e) Barltrop, J. A.; Carless, H. A. J. *J. Am. Chem. Soc.* **1972**, *94*, 8761. (f) Wagner, P. J.; Kochevar, I. *J. Am. Chem. Soc.* **1969**, *90*, 2232.

(12) large number of biologically active compounds possessing the imidazolidine-4,5-dione moiety have been reported (a) Arafa, R. K.; Nour, M. S.; El-Sayed, N. A. *Eur. J. Med. Chem.* **2013**, *69*, 498. (b) Abou-Seri, S. M.; Farag, N. A.; Hassan, G. S. *Chem. Pharm. Bull.* **2011**, *59*, 1124. (c) Xia, G.; Benmohamed, R.; Kim, J.; Arvanites, A. C.; Morimoto, R. I.; Ferrante, R. J.; Kirsch, D. R.; Silverman, R. B. *J. Med. Chem.* **2011**, *54*, 2409. (d) Rajabi, M.; Mansell, D.; Freeman, S.; Bryce, R. *Eur. J. Med. Chem.* **2011**, *46*, 1165. (e) Guan, J.; Wang, X.; Smith, K.; Ager, A.; Gettayacamin, M.; Kyle, D. E.; Milhous, W. K.; Kozar, M. P.; Magill, A. J.; Lin, A. J. *J. Med. Chem.* **2007**, *50*, 6226.

(13) Overall ten products were characterized by x-ray analysis. Non-crystalline compounds were characterized by solution NMR and their structure confirmed with the help of *DU8+* NMR computations described in ref. 14.

(14) (a) Kutateladze, A. G.; Reddy, D. S. *J. Org. Chem.*, **2017**, *82*, 3368 (b) Kutateladze, A. G.; Mukhina, O. A. *J. Org. Chem.* **2015**, *80*, 10838. (c) Kutateladze, A. G.; Mukhina, O. A. *J. Org. Chem.*, **2015**, *80*, 5218. (d) Kutateladze, A. G.; Mukhina, O. A. *J. Org. Chem.* **2014**, *79*, 8397.

(15) (a) Truhlar, D. G.; Gao, J.; Alhambra, C.; Garcia-Viloca, M.; Corchado, J.; Sanchez, M. L.; Villa, J. *Acc. Chem. Res.* **2002**, *35*, 341. (b) Basran, J.; Sutcliffe, M. J.; Scrutton, N. S. *Biochemistry*, **1999**, *38*, 3218. (c) Brooks, H. B.; Jones, L. H.; Davidson, V. L. *Biochemistry* **1993**, *32*, 2725.

(16) (a) Garcia-Garibay, M. A.; Gamarnik, A.; Pang, L.; Jenks, W. S. *J. Am. Chem. Soc.* **1994**, *116*, 12095. (b) Garcia-Garibay, M. A.; Gamarnik, A.; Bise, R.; Pang, L.; Jenks, W. S. *J. Am. Chem. Soc.* **1995**, *117*, 10264. (c) Johnson, B. A.; Gamarnik A.; Garcia-Garibay, M. A. *J. Phys. Chem.* **1996**, *100*, 4697. (d) Gamarnik, A.; Johnson, B. A.; Garcia-Garibay, M. A. *J. Phys. Chem. A.*, **1998**, *102,* 5491. (e) Johnson, B. A.; Kleinman, M. H.; Turro, N. J.; Garcia-Garibay, M. A. *J. Org. Chem.* **2002**, *67*, 6944.

(17) (a) Caremella, P.; Cellerino, G.; Coda, A. C.; Invernizzi, A. G.; Grunanger, P.; Houk K. N.; Albini, F. M. *J. Org. Chem.* **1976**, *41*, 3349. (b)Wang, J.-F.; Wang, J.-F. Wei, D.-Q.; Wang, C.-F.; Ye, Y.; Li, Y.-X., Luo, Y.; Wang, W.-W.; Liu, L.-Z.; Zhao, Y.-F. *J. Theor. Comp. Chem.* **2007**, 6, 861. (c) Rossbach, J.; Harms, K.; Koert, U. *Org. Lett.* **2015**, *17*, 3122. (d) Kesornpun, C.; Aree, T.; Mahidol, C.; Ruchirawat, S.; Kittakoop, P. *Angew. Chem. Int. Ed.* **2016**, *55*, 3997.

(18) Vatsadze, S. Z.; Loginova, Y. D.; Gomes, G. d. P.; Alabugin I. V. *Chem. Eur. J.* **2017**, *23*, 3225.

TOC GRAPHIC

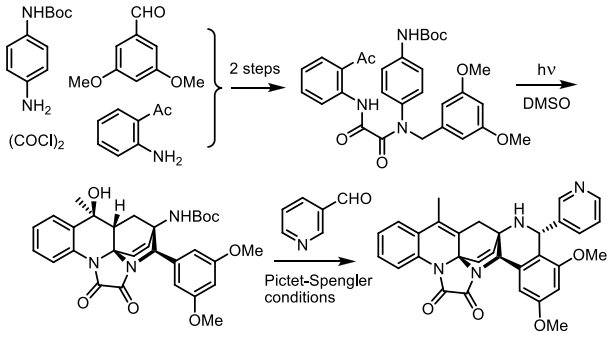
NHBoc
CHO
MeO
OMe
NH2
(COCl)2
Ac
NH2
2 steps
NHBoc
Ac
NH
OMe
N
OMe
O
O
hν
DMSO
OH
H
NHBoc
N
N
O
O
OMe
OMe
CHO
N
Pictet-Spengler
conditions
N
H
N
N
O
O
OMe
OMe